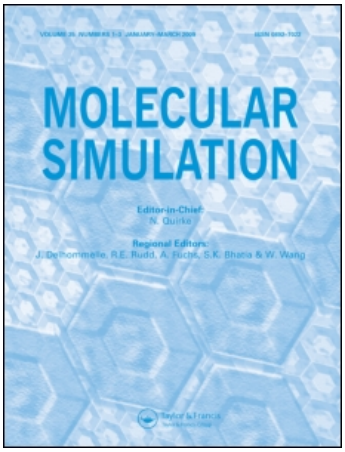

Molecular Simulation
Publication details, including instructions for authors and subscription information:
http://www.informaworld.com/smpp/title~content=t713644482

Equilibrium Properties of a Charged Polymer Chain with Short Range Interactions

J. Takashima[a]; M. Takasu[a]; Y. Hiwatari[a]
[a] Department of Physics, Faculty of Science, Kanazawa University, Kanazawa, Japan

To cite this Article Takashima, J. , Takasu, M. and Hiwatari, Y.(1991) 'Equilibrium Properties of a Charged Polymer Chain with Short Range Interactions', Molecular Simulation, 6: 4, 199 — 220
To link to this Article: DOI: 10.1080/08927029108022429
URL: http://dx.doi.org/10.1080/08927029108022429

Molecular Simulation, 1991, Vol. 6, pp. 199–220
Reprints available directly from the publisher
Photocopying permitted by license only

EQUILIBRIUM PROPERTIES OF A CHARGED POLYMER CHAIN WITH SHORT RANGE INTERACTIONS: TWO-DIMENSIONAL MONTE CARLO STUDIES

J. TAKASHIMA, M. TAKASU and Y. HIWATARI

Department of Physics, Faculty of Science, Kanazawa University, Kanazawa 920, Japan

(*Received May 1990, accepted June 1990*)

We study the equilibrium properties of a two-dimensional charged polymer with screened Coulomb interactions by Monte Carlo simulations on a two-lattice model. It is found that the local conformation of the polymer is substantially dependent on the range of the interaction between the ions of the monomers and their counterions. The scaling relation for the gyration radius of the neutral polymer works also for the charged polymer. It is suggested that the Flory exponent shows a temperature dependent behavior at low temperatures. The segment analysis was also made to obtain that the end segment dominates the average properties of the finite size polymer.

KEY WORDS: Charged polymer, polyelectrolyte, gyration radius, winding angle, Monte Carlo simulation.

1. INTRODUCTION

Charged polymers [1–7] have attracted much attention in many areas, such as engineering, medicine and pharmacy. The equilibrium properties of a charged polymer are supposed to be much more complex than a neutral polymer, because of the existence of Coulomb interactions between the monomer ions on the polymer and their counterions. For the latter, considerable knowledge has already been accumulated.

In this paper, we consider a simple model for a charged polymer chain in a solution with two-dimensional square lattices, on which monomers of the polymer chain and the counterions move. All ions interact via screened Coulomb potentials. The details of the Monte Carlo simulations, the method of generating of the samples and the model lattice which we used, are explained in the following Section.

We report on our calculations of the gyration radius R_G, and mean length of turns S, and discuss the effect of the range of interactions between ions. R_G measures the global conformation of the polymer chain, while S does the local property.

We also report on the winding angle θ. For a uncharged polymer chain (neutral polymer), Duplantier and Saleur [8] proved, by the conformation field theory, that the distribution of θ obeys the following Gaussian form.

$$p(x) \sim \pi^{-1/2} \exp(-x^2) \qquad \text{for } N \to \infty \tag{1}$$

where $x = (4 \ln N)^{-1/2} \theta$ and N the length of the self-avoiding walk. In this work, we study the same distribution for a charged polymer chain.

With the help of segment-division analyses, we see that some of the equilibrium properties of the polymer chain are well correlated with the end-segment properties, which may differ from those of inner segments, although such end effects should disappear for a thermodynamic limit (infinite N).

2. MONTE CARLO CALCULATIONS

2.1 Model for a Charged Polymer Chain

Often a polymer chain is composed of monomers (repeated units) with a group of molecules. These monomers are usually much smaller than an entire polymer chain in size and length. The bond between adjacent monomers is called link. There are various types of polymers, but here we consider a polymer chain as simple as possible such that it has a single repeated monomer, and no branch point.

Suppose that each monomer is charged by $-$ under ionization when a charged polymer chain dissolves in a good solvent at high temperatures. Consequently a polymer carries charge $-(N+1)q$, where $(N+1)$ is the number of monomers of the chain. An electrically neutral condition yields an appearance of an equal number of counterions with an opposite charge $(+q)$. The equlibrium properties of a charged polymer chain differ from a neutral polymer chain in many respects due to the Coulomb interactions between the monomers and counterions. For example, at low temperatures, the counterions tend to be recombined by the monomers due to the Coulomb attraction. This phenomenon is called a condensation of counterions, which results in decreasing the effective total charge of the polymer chain, but produces dipole polarizations at monomer sites at the same time to have an effect on the chain conformation.

In order to investigate fundamental properties characteristic to such a charged polymer chain, we study a simple two-dimensional lattice model for a polymer chain with Monte Carlo simulations. We describe the details of our Monte Carlo calculations below.

2.2. Interactions

We employ a square lattice model: monomers and counterions are restricted to move on vacant sites on an assumed lattice, single square lattice or two-square-lattice as described below. When a certain lattice site is already occupied by one ion (monomer or counterion), the other ions are prohibited to come to this site due to the excluded volume effect. We put the lattice spacing equal to the length of link (bond length), which is also used as the units of the length throughout this paper. The polymer chain lies on the net of the lattice, so that the angle between the successive links is restricted to be 0 or ± 90 degrees in the present model. Each counterion takes one of unoccupied lattice points by either monomers or other counterions, of which available site depend on the lattice model adopted.

The Monte Carlo simulations have been made on a square cell with a side length of L. The periodic boundary conditions are imposed as usual. A single chain composed of $N+1$ monomers and $N+1$ counterions are contained in the simulation cell. We consider a dilute system satisfying that $L \geqq N+1$. We have carried out Monte Carlo simulations for five different sizes of the chain, up to the maximum chain length of $N+1=200$, and set the counterion concentration to be $(N+1)/$

$L^2 = 0.005$ throughout this work: $(N + 1, L) = (18,60)$, $(32,80)$, $(50,100)$, $(98,140)$, and $(200,200)$.

For the interaction between ions, we assumed the screened Coulomb interaction shown below as well as the excluded volume interaction that can be taken into account by a simple procedure avoiding the double-occupancy of any ions in the same lattice site as mentioned above. In our two-dimensional model, we use a logarithmic potential with a cut-off length r_c due to the screening effects by assumed added salts ions, which are, however, not taken into considerations explicitly in our simulations. Thus, the interactions between any pair of ions, i and j, are assumed to be:

$$\begin{aligned} v_{ij}(r) &= +\infty, && (r = 0) \\ &\quad -q_i q_j C \ln(r/l), && (0 < r \leqq r_c) \\ &\quad 0, && (r > r_c) \end{aligned} \tag{2}$$

where the first equation represents the excluded volume effect, and the second and third equations are Coulomb interactions with a cut-off length r_c. Here we set $q_i = 1$ for the monomers, $q_i = -1$ for the counterions, and r is the distance between two ions. C and l are positive constants, the values of which are determined in the following Section.

2.3. *Slithering Snake Method*

It is not as simple as in the simulations of free atoms to simulate the movement of monomers on a chain, to be satisfied by the constraint at any Monte Carlo step such that each monomer is linked (bonded) by the respective neighboring monomers. In the present lattice model, the length of all links is fixed to be equal to the lattice

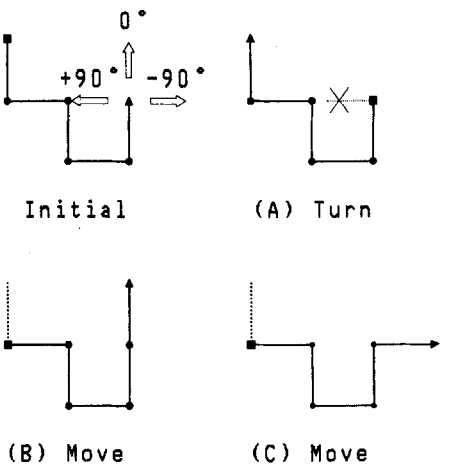

Figure 1 Schematic diagrams of the slithering snake method. The closed triangle and closed box represent the head and the tail of the chain, respectively, and closed circles are other monomers. With a Monte Carlo trial the initial chain selects three directions shown by arrows. If that direction is left (+90 deg.), the chain turns by exchanging the head and tail because of the excluded volume (A). When either of other two directions (forward and right) is selected, the chain moves one step to generate a new chain configuration (B or C).

constant. While both end monomers are able to move almost freely, inner monomers are rather difficult to move due to the above constraint. For the Monte Carlo simulations of this specific system, the slithering snake method turns out to be very useful [9]. In this work we employ this method and study the equilibrium properties, including the global and local conformation characteristics of a charged polymer chain and the scaling properties that have been proposed for a neutral chain.

As an initial configuration of the chain, we use an arbitrary chain configuration. One end of the chain is named as 'head' and the other end of the chain as the 'tail'. In the slithering snake method, the tail monomer is cut and linked to the head monomer at a randomly selected site of the nearest neighbors of the head. In the square lattice, there are three possible sites for the head monomer movement towards left (90 deg.), forward (0 deg.), or right (-90 deg.) directions, as shown in an example of Figure 1. This movement is equivalent, just as in a slithering snake motion, to a translational motion of all monomers except the head monomer, by the distance of the lattice constant along the chain, accompanied by the head motion to the direction selected as in the above way. By this way, a trial chain configuration is generated. The energy of this trial configuration is calculated and compared with the original one to determine the former either to be accepted or rejected as a new configuration using a usual Metropolis method [10]. When accepted, the trial configuration is replaced with the original configuration as a new configuration for the next Monte Carlo step. On the other hand, when rejected, the head and tail of the original chain are exchanged, and this is used as a new configuration. Thus we generate successive chain configurations, by repeating this procedure until a enough number of samples are obtained.

2.4. The problem of Cul-de-sacs and Refresh Cycle

The slithering snake method mentioned above turns out to be a very effective way to obtain statistically independent samples for the chain configuration at any temperatures, simply and more quickly than other methods like the self-avoiding walk, especially for long chains. There are two points to be noted in this method. One is so-called cul-de-sac problem which may more frequently take place in a two-dimensional case than in a three-dimensional case. When the head of the chain is in a cul-de-sac, the chain is not able to move along this direction, and consequently the chain is obliged to exchange the head with the tail to escape from the cul-de-sac. But if the tail is occasionally in a cul-de-sac at the same time, the chain has no freedom to move any more. Therefore, all samples generated afterward must be the same. However, except for the special case that an initial chain configuration is in cul-de-sac at either end of the chain, the chain never gets into cul-de-sacs at both ends at the same time in any Monte Carlo steps with the slithering snake method, because of the principle of the reversibility of Monte Carlo processes. Thus, provided that we could avoid such a special initial conformation, the slithering snake method will work without this problem, which is in general possible.

The other point is about sampling correlations. The difference between the original and updated chain configurations at any Monte Carlo step is at most by only one link position at either end of the chain, since the other links remain unchanged and the turn of the chain direction (exchange of the head and tail) changes nothing about the configuration. Supposing that the chain continues to move without turns, the chain could be refreshed completely after N steps. However, due to frequent turns of the

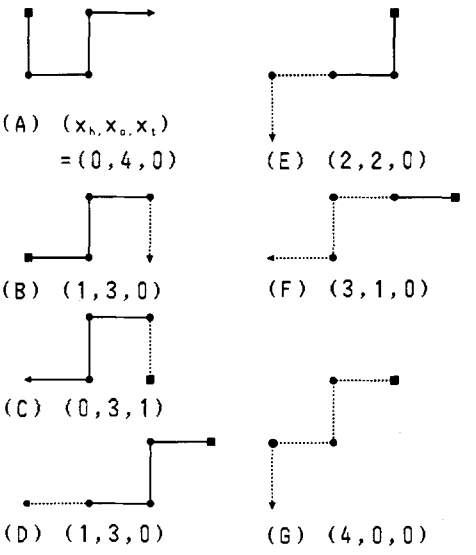

Figure 2 Schematic representations for the refresh cycle-time calcuation. The closed triangle and closed box denote the head and tail of the chain, respectively, and closed circles are other monomers. The solid lines denote the initial links, and the dashed lines denote the refreshed links: Let (A) denote the initial chain conformation for $N + 1 = 5$, and the chain conformation changes from (A) to (G) following next six Monte Carlo steps. In this example the initial chain is completely refreshed by 6 steps (5 moves and 1 turn) in (G).

chain during Monte Carlo steps, it takes much more steps for the chain configuration to be refreshed completely. We have calculated the number of time steps necessary to refresh the chain as follows.

Start with a configuration given with N links at an initial Monte Carlo time. Following subsequent Monte Carlo steps, links existent in the initial configuration disappear step by step through the successive procedures of cutting the tail and putting it together at the head of the chain to produce a new link on the chain. Let us introduce x_h and x_t which denote a number of links refreshed at the head and tail in the chain, respectively, by the present Monte Carlo step (see Figure 2). Then, $x_0 = N - (x_h + x_t)$ means the number of links remaining unchanged so far. At the initial time, $x_h = x_t = 0$ and $x_0 = N$. As the chain moves by one step, x_h becomes $x_h + 1$, whereas x_t becomes $x_t - 1$, only when $x_t > 0$. On the other hand, when the chain interchanges the head and tail, the value of x_h and x_t are interchanged, and x_0 remains unchanged. According to this procedure, the chain can be refreshed completely, namely $x_0 = 0$, after a number of Monte Carlo steps. We show an example in Figure 2.

We call the number of steps of both moves and turns necessary for the chain to be refreshed completely the 'Refresh Cycle', T_r. T_r differs from the correlation factor introduced by Mandel [9], in which the number of turns are not taken into considerations. Over every T_r, updated Monte Carlo samples may be regarded as to be statistically uncorrelated to the former sample, that is, correlations between two samples should be lost. In order to obtain an equilibrium state at any temperature, Monte Carlo simulations over many times of the refresh cycle are required. The

refresh cycle time strongly depends on the temperature of the system; for lower temperature it becomes longer. Thus, the refresh cycle is an important parameter to the slithering snake simulation.

2.5. *Single-Lattice Model*

First, we use the single-lattice model in order to study the equilibrium properties of the polymer chain. This model has the difficulty of simulating a low temperature polymer chain as mentioned below, but has a great advantage of the simplicity. Therefore we consider this lattice model first. Let us consider a square lattice with $L \times L$ sites, and put a single chain ($N + 1$ monomers) along the lattice and $N + 1$ counterions on the lattice sites, taking into consideration of the double occupancy avoidance for any ions. This means that if a chain has a length of the same order of magnitude as the side length of the cell, the chain partitions counterions into both sides of the chain, since no counterions are able to cross a chain. As another

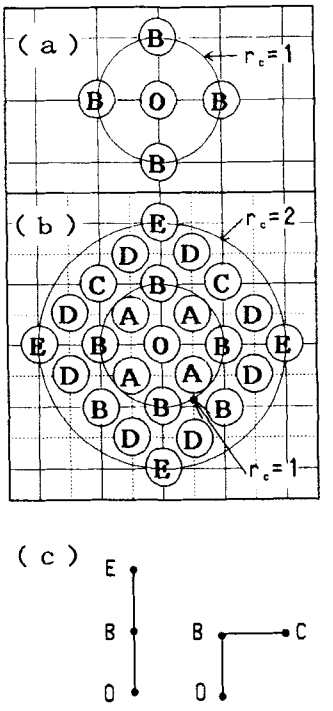

Figure 3 Schematic representations of the lattice model and cutoff length r_c, (a) $r_c = 1$ with the single-lattice model, (b) $r_c = 1$ and $r_c = 2$ with the two-lattice model (inner circle and outer circle, respectively). In (c), examples of local chain configuration of the successive two links are shown. For the model (a), the polymer and counterions move on the same square lattice. Suppose that the center site O is occupied by a monomer. It interacts with B sites only. On the other hand, for the model (b), the polymer moves on the lattice denoted by the solid lines, but counterions move on another lattice denoted by the dashed lines. The monomer occupying O site interacts with A to E sites, depending on the choice of r_c. A and D are sites for counterions; B, C, and E are for monomers.

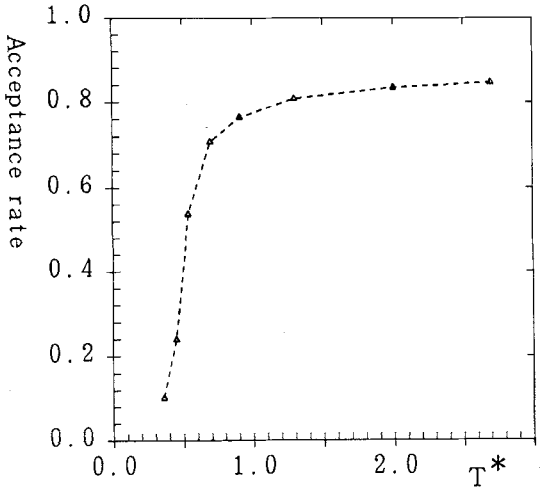

Figure 4 The temperature dependence of the acceptance rate for the chain movement with the single-lattice model for $r_c = 1$. The dashed curve is drawn as a guide to the eyes.

disadvantage of this model it may happen that counterions near the head of the chain block the chain motions, especially at low temperatures.

In a strong screening regime, we can use a nearest-neighbor approximation, by setting the cut-off length to be $r_c = 1$ in Equation (2), as shown in Figure 3(a). As the units of energy we use ε, the interaction energy between a monomer and a counterion at the nearest-neighbor distance, and as the reduced temperature T^*:

$$\begin{aligned} \varepsilon &= v(1) \\ T^* &= k_B T/\varepsilon \end{aligned} \tag{3}$$

where $v(r)$ is the same as Equation (2), and k_B denotes the Boltzmann constant.

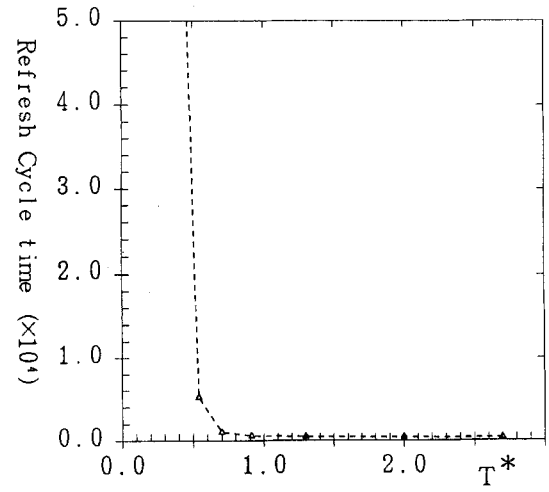

Figure 5 The temperature dependence of the refresh cycle time with the single-lattice model for $r_c = 1$. The dashed curve is drawn as a guide to the eyes.

We studied $N + 1 = 50$ chain with a single-square lattice model via Monte Carlo simulations. The acceptance rate is shown in Figure 4. At high temperatures, it shows a high acceptance rate, whereas it decreases rapidly at low temperatures, implying a difficulty of the simulations. The refresh cycle time is shown in Figure 5. At low temperatures below $T^* = 0.5$, it becomes very long: for example, the refresh cycle time reaches of an order of 10^6 steps at $T^* = 0.36$. A low acceptance rate and a large refresh-cycle time are caused mainly from frequent cul-de-sacs problems at the head of the chain. The reason for such a cul-de-sac is the appearance of condensed counterions near the head of the chain, which obstruct the motion of the chain. As a result, the chain repeats turning head and tail at many time steps, trying to move from the near-neighbor counterions around the head of the chain, which is rather unnatural, in contradiction to the attractions between the head monomer charge and the near-neighbor counterions.

2.6. *Two-lattice Model*

As a way of reducing the problems which we have seen above we propose the two-lattice model: of two square sub-lattices with $L \times L$ sites each, one is used for a polymer chain (monomers), and the other for counterions. Similar to the single-lattice model, the ions move on either lattice sites and the double occupancy at the same site is prohibited. In this model, any counterion site has four nearest monomer sites, and any monomer site has four nearest counterion sites. Unlike the single-lattice model, neither the counterions are partitioned by the chain, so that the counterions are able to cross the chain, nor the motion of the head of the chain is blocked by the near-neighbor counterions. The chain is able to slither even if the chain head is surrounded by counterions. Therefore no contradiction will take place which arises in the single-lattice model, as mentioned above. Thus, the two-lattice model substantially overcomes the faults of the single-lattice model.

There is another advantage of the two-lattice model that the counterions are able to approach the monomers more closely than in the single-lattice model. As a consequence, it is possible in the two-lattice model that many counterions can be at the nearest neighbor distance from more monomers than those for the single-lattice model. This brings the condensation in the present model to be more stable than in the single-lattice model at low temperatures. Furthermore, the directions of the dipoles at monomer sites, which differ for the models used, will influence the statistical properties of the chain in a complicated way. We have carried out Monte Carlo simulations for a charged polymer chain using the two-square-lattice model.

Table 1 The value of the Coulomb energy at the respective near-neighbor distance and potential parameters used in the present two-lattice model. Lattice spacing is used as the unit of the length, and ε as the unit of the energy, which is the absolute value of the Coulomb energy for a pair of monomer and nearest-neighbor counterion, namely $\varepsilon = |v(r = 0.707)|$. Constant l in $v(r)$ is fixed arbitrarily to satisfy the condition that the discontinuity of $v(r)$ at $r = r_c$ becomes small. The pairs of sites OA $\sim$ OE are shown in Figure 3(b).

Pair of sites		$v(r)/\varepsilon$ *O-A*	*O-B*	*O-C*	*O-D*	*O-E*
r		0.707	1.000	1.414	1.581	2.000
(a)$r_c = 1$	$l = 1.495$	−1.000	0.537	–	–	–
(b)$r_c = 2$	$l = 2.121$	−1.000	0.685	0.369	−0.268	0.054

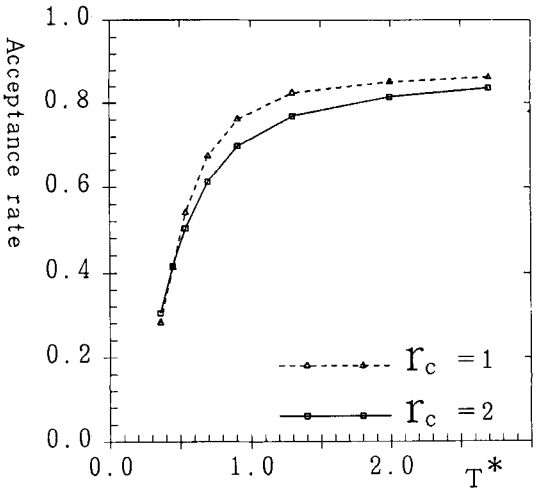

Figure 6 The temperature dependence of the acceptance rate for the chain movement with the two-lattice model. △ is for $r_c = 1$, and □ is for $r_c = 2$. Each curve is drawn as a guide to the eyes.

We have studied two cases of the range of interactions between monomers and counterions. One is the nearest-neighbor approximation (cut-off length $r_c = 1$), and the other is the third-nearest-neighbor approximation ($r_c = 2$) (see Figure 3(b) and Table 1).

The most important difference between both cases, $r_c = 1$ and $r_c = 2$, is of the interaction energy between three successive monomers. In Figure 3(c), we give an example of two different configurations, OBC and OBE. In the case of $r_c = 1$, there is no energy difference between these two conformations, while in the case of $r_c = 2$,

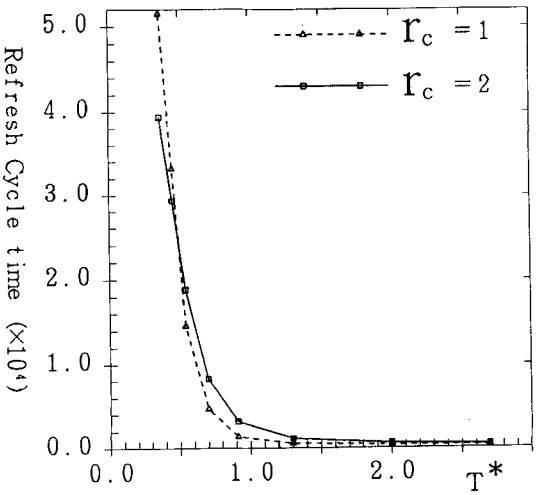

Figure 7 The temperature dependence of the refresh cycle time with the two-lattice model. △ is for $r_c = 1$, and □ is for $r_c = 2$. Each curve is drawn as a guide to the eyes.

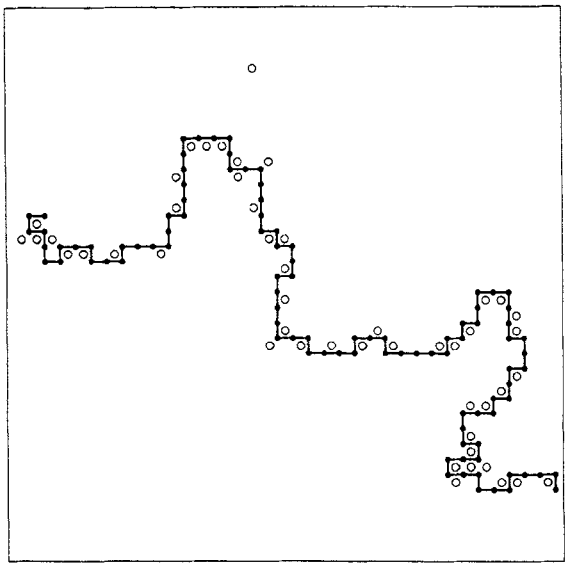

Figure 8 Snapshot chain configuration obtained by the present Monte Carlo simulations for $N + 1 = 98$, $T^* = 0.36$, and $r_c = 2$. The solid line with dots on it represents the chain, monomers are represented by dots. The white circles are the counterions.

OBC has a larger energy than OBE due to the repulsion between O and C. Therefore, in the case of $r_c = 2$, the chain is more likely to take a rodlike local conformation.

In this model, a charge condensation is identified by a pair of a counterion and a monomer at a distance of $2^{-1/2}$. We define ε as the unit energy and T^* as the reduced temperature:

$$\begin{aligned} \varepsilon &= v(2^{-1/2}) \\ T^* &= k_B T/\varepsilon \end{aligned} \tag{4}$$

We have studied the acceptance rate and refresh cycle time for the chain of $N + 1 = 50$ with the two-lattice model. The acceptance rate is shown in Figure 6. A better acceptance rate is obtained than in the single-lattice model (Figure 4) at low temperatures. The refresh cycle time is shown in Figure 7. It should be notable that the cycle time at low temperatures becomes much smaller than that in the single-lattice model shown in Figure 5. The refresh cycle time is proportional to the square of the chain length [9]. Since the refresh cycle time is of an order of $T_r = 5 \times 10^4$ for $N + 1 = 50$, it becomes of an order of $T_r = 8 \times 10^5$ for $N + 1 = 200$, which is large, but a feasible number in usual Monte Carlo simulations. An example of the chain conformation obtained by the present Monte Carlo calculations is given in Figure 8. We see that overall condensations of the counterions take place at the lowest temperature. In the next Section, we discuss the conformation characteristics of the charged polymer chain in detail and the scaling property in comparison with those of a neutral polymer chain.

3 RESULTS

3.1. Effective Charge and Internal Energy

The Monte Carlo simulation was initiated with an arbitrary configuration of a single chain ($N + 1$ monomers) and an equal number of counterions in a two-dimensional double-square lattice. We define one Monte Carlo step by one slithering snake trial and $N + 1$ trials of the counterions. The simulations were carried out over the time steps of an order of $10^6 \sim 10^7$ at a sufficiently high temperature, and the last configuration was used as an initial configuration for a given lower temperature. This process was repeated to obtain further low-temperature samples, for each of which $10^6 \sim 10^7$ configurations were simulated.

The net charge of the polymer chain is $-(N + 1)q$, since each monomer carries a charge $-q$. When N_c counterions are condensed on the polymer chain, the effective net charge of the polymer chain is reduced to $[N_c - (N + 1)]q$. Thus, the condensation cancels the net polymer charge, and the effective charge per unit monomer decreases. The effective charge Q^* is therefore defined as:

$$Q^* = 1 - N_c/(N + 1) \tag{5}$$

From Equation (2), the total potential energy per unit monomer is calculated by

$$U^* = \frac{1}{2\varepsilon(N + 1)} \sum_i \sum_j v_{ij}(r) - \frac{Nv(1)}{\varepsilon(N + 1)} \tag{6}$$

where the second term, equal to the Coulomb energy of monomer pairs at the nearest neighbor (bond) distance, was used as the origin of the energy. The summation is made over all ion pairs of monomers and counterions.

The temperature dependence of Q^* and U^* are shown in Figure 9 and Figure 10, respectively. There is no significant size dependence for either Q^* or U^*. We note that the curves shown there exhibit little temperature dependence above $T^* \sim 1$. However, they fall rapidly as the temperature is lowered below $T^* \sim 1$. From these

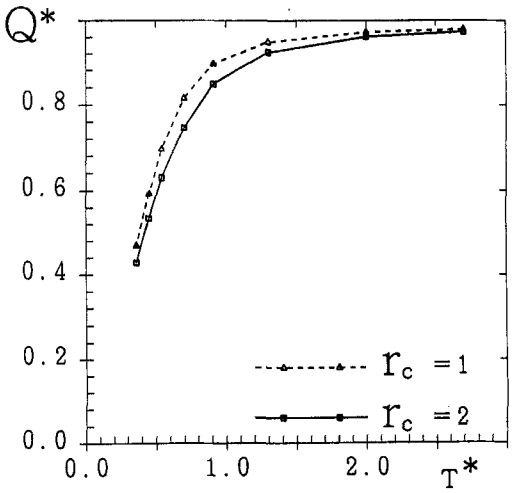

Figure 9 The temperature dependence of Q^*. △ is for $r_c = 1$, and □ is for $r_c = 2$. Each curve is drawn as a guide to the eyes.

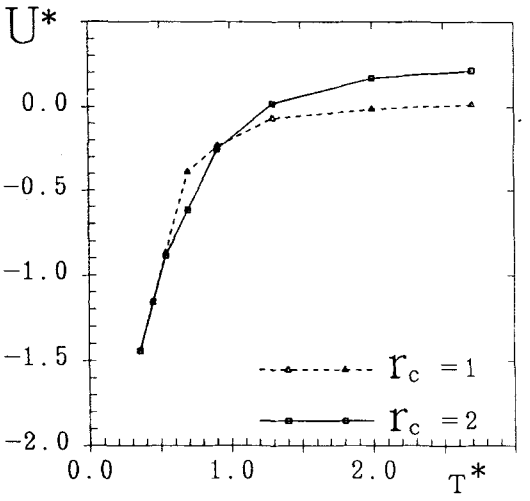

Figure 10 The temperature dependence of U^*. △ is for $r_c = 1$, and □ is for $r_c = 2$. Each curve is drawn as a guide to the eyes.

behaviors, we may predict that there are two distinguishable phases, the high-temperature ionized phase and low-temperature condensed phase. In the high-temperature phase ($T^* > 1$), most of the counterions are distant from the chain, and consequently it follows that $Q^* \sim 1$ for both $r_c = 1$ and $r_c = 2$. As a result, U^* is dominated by the repulsive potential energy between monomers. Due to extremely short range interactions for $r_c = 1$, it follows that $U^* = 0$. For $r_c = 2$, however, U^* provides a positive value, which mainly results from the next-nearest-neighbor monomer-monomer interactions.

On the other hand, in the low-temperature phase ($T^* < 1$), as counterions are condensed (Q^* decreases rapidly), U^* becomes small because of the attractive potential energy between monomers and condensed counterions. We note that there is no cross point of the curves in Q^*, while it happens in U^* around $T^* = 1$. This suggests that the local conformation characteristics of the chain will significantly differ between two models, which we will study in detail below.

3.2. Global Conformation and Local Conformation

In order to study the global conformation characteristics of the polymer chain, the radius of gyration R_G has been calculated. R_G is defined by

$$R_G^2 = \frac{1}{2(N+1)^2} \sum_i \sum_j \langle | \mathbf{r}_i - \mathbf{r}_j |^2 \rangle \tag{7}$$

where r_i denotes the position vector of the i-th monomer, and the summation is made over all pairs of monomers.

R_G measures a global extension of the chain, which is substantially influenced by the monomer-monomer repulsion and the monomer-counterion attraction. It is well known that R_G follows the following scaling law [11] for a neutral monomer:

$$R_G \sim N^{\nu} \tag{8}$$

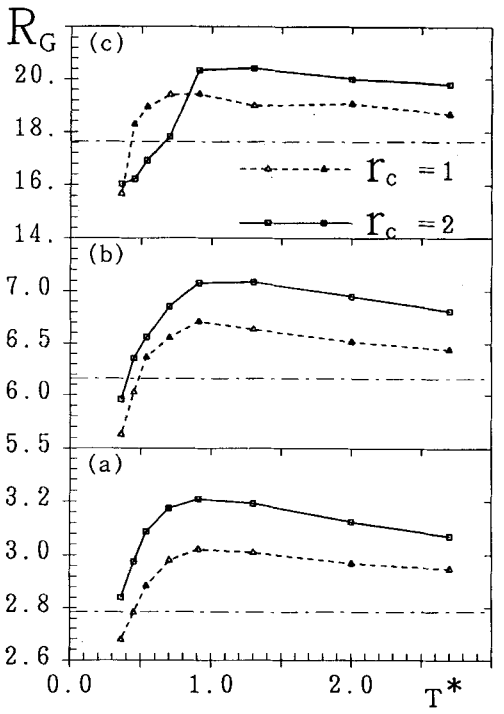

Figure 11 The temperature dependence of R_G for (a) $N + 1 = 18$, (b) $N + 1 = 50$, and (c) $N + 1 = 200$. △ is for $r_c = 1$, and □ is for $r_c = 2$. Each curve is drawn as a guide to the eyes. The value of R_G for the neutral polymer chain is shown by dash-dotted line: $R_G \sim$ (a) 2.78, (b) 6.17, and (c) 17.6.

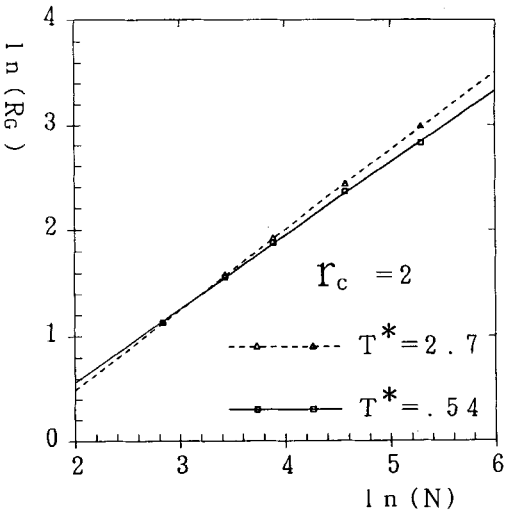

Figure 12 The plots of $\ln(R_G)$ vs. $\ln(N)$ at $T^* = 2.7$ (△) and $T^* = 0.54$ (□) for $r_c = 2$. Each line is obtained by a least-square fitting.

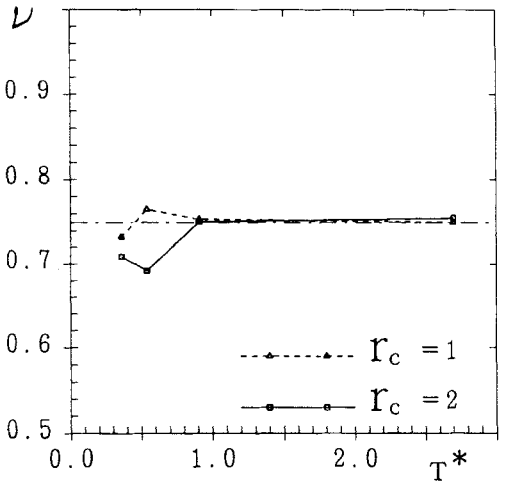

Figure 13 The temperature dependence of Flory exponent υ for $r_c = 1$ (△) and for $r_c = 2$ (□). Each curve is drawn as a guide to the eyes. Dash-dotted line shows the value of υ for the neutral polymer chain.

with the Flory exponent υ. The value of υ depends on the dimensionality of the system as well as the model under consideration. For a neutral polymer chain in two dimension, υ is 0.75 when the excluded volume effect is taken into consideration (self-avoiding-walk), whereas υ is 0.5 without it (random-walk). In general, it holds that $0.5 \leqq \upsilon \leqq 1$ in two dimension. The lower-limit condition, $\upsilon = 0.5$, is realized when the chain is formed to be a "closed packed" conformation (minimum packed). The upper-limit condition, $\upsilon = 1$, to be a rodlike conformation (line packed). Then, we call the chain to be rodlike when $\upsilon > 0.75$, and "closed packed" when $\upsilon < 0.75$.

The temperature dependence of R_G is shown in Figure 11 for different lengths of the chain. It is noted that the peak appears around $T^* = 1$ for both $r_c = 1$ and $r_c = 2$. R_G decreases rapidly at lower temperatures, indicating that a global contraction of the chain takes place remarkably below $T^* = 1$. There is no size dependence of R_G for $r_c = 1$. For $r_c = 2$, however, R_G shows a remarkable N-dependence. As N becomes larger, the following behaviors are observed. First, at right-hand side of the peak (the high-temperature phase), the value of R_G seems to decrease more gradually. Secondly, at left-hand side (the low-temperature phase), R_G seems to decrease more rapidly. These behaviors indicate that the change of R_G around $T^* = 1$ becomes sharper as the polymer chain becomes longer. Thus, if the chain is long enough, a sharp change may be observed.

From the value of R_G for various chain lengths, we have plotted $\ln(R_G)$ vs. $\ln(N)$ in Figure 12. For both temperatures $T^* = 2.7$ and 0.54, R_G satisfies the scaling relation Equation (8). For other temperatures, similar results are obtained, as well. Therefore, we conclude that the scaling property is well satisfied in the present model, too. We obtain the Flory exponent υ, the temperature dependence of which is shown in Figure 13. As expected, at high temperatures, υ is equal to that of the neutral polymer chain within the statistical accuracy of the present calculations. Monomer-monomer repulsion has no influence upon the Flory exponent at high temperatures. But at low temperatures, our result shows that υ is not constant, yielding significant deviation from 0.75. "The Flory exponent" υ depends on the temperature and the

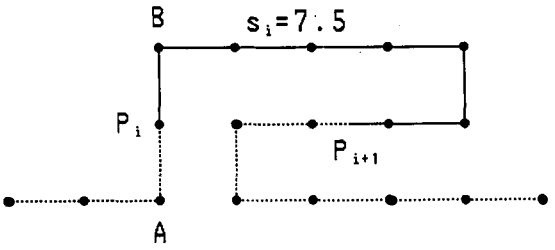

Figure 14 Schematic diagram for S. The inflection point is defined as the middle point between the two bend points, which have different turning directions with each other. For example, P_i is the middle point of A and B. The section s_i is measured along the chain.

range of interaction. In the case of $r_c = 1$, as the temperature is lowered, υ increases up to 0.765 at $T^* = 0.54$ and decreases down to 0.732 at $T^* = 0.36$. On the other hand, in the case of $R_c = 2$, υ decreases down to 0.692 at $T^* = 0.54$ and increases again up to 0.709 at $T^* = 0.36$.

In the following, we study the local conformation characteristics of the polymer chain. As in our previous paper [5], we introduce a quantity S, that is, the average length of turns of the chain:

$$S = \left\langle \frac{1}{K-1} \sum_{i=1}^{K-1} s_i \right\rangle \tag{9}$$

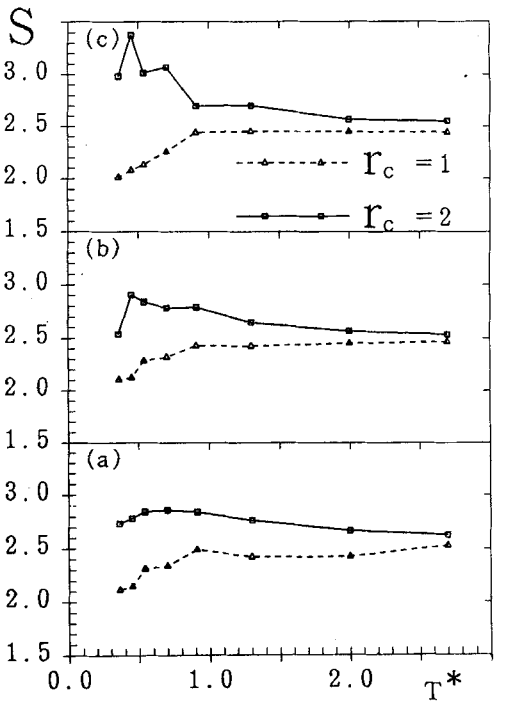

Figure 15 The temperature dependence of S for (a) $N + 1 = 18$, (b) $N + 1 = 50$, and (c) $N + 1 = 200$. Δ is for $r_c = 1$, and $\square$ is for $r_c = 2$. Each curve is drawn as a guide to the eyes.

where s_i denotes the curvilinear distance between the $(i + 1)$th and i-th inflection points, and K is the total number of the inflection points of the chain (see Figure 14). In this calculation, we omitted both s_0 and s_N at either side of the chain. S measures the degree of local chain stiffness: S becomes large for a stiff chain, and small for a soft chain. The temperature dependence of S is shown in Figure 15. In the case of $r_c = 1$, little N-dependence is observed. S begins to decrease as the temperature is lowered below $T^* = 1$. In the case of $r_c = 2$, there is a maximum in the curve of S around $T^* = 0.5$ for $N + 1 = 50$ and $N + 1 = 200$, and the maximum value is higher for larger N. Below $T^* = 0.5$, S decreases again as the temperature is lowered. It is the result of the strong charge condensation, which makes the chain less stiff.

The overall properties of R_G and S obtained in the present work makes it possible to summarize as follows about the conformation characteristics of the charged polymer chain, from global and local viewpoints. For the nearest-neighbor approximation ($r_c = 1$), the result which we have obtained is similar to that of the single square-lattice model studied by Victor *et al.* [1]; neither R_G nor S shows any significant N dependence, and both show a similar temperature dependence. There are little difference of the global and local conformation characteristics of the chain between two models. On the other hand, for the third-nearest-neighbor approximation ($r_c = 2$), the conformation characteristics of the polymer chain are found to be significantly different from those of the nearest-neighbor approximation ($r_c = 1$). The temperature dependence of R_G notably differs from that of S. As soon as the counterions begin to condense ($T^* \sim 1$), R_G decreases rapidly, but S increases until it tends to decrease for further decreasing temperatures, when most counterions are condensed. This behavior indicates that, as the temperature is lowered below $T^* = 1$, the chain contracts globally, but it is stiffened locally. v takes the minimum value for this "transition" temperature.

3.3. Segment-Division Analysis

When a chain is long, the properties of the end parts of the chain should be different from those of the inner parts of the chain. In this section, we make segment-division analyses for the chain.

We take a chain of $N + 1 = 98$. First, the chain is divided into two-equal parts (the head part and the tail part). Because of the symmetry, both parts should have the same conformation characteristics. Therefore, we only have to consider a half chain with inner monomers at one side and end monomers at the other side. The half chain is further divided into six equal segments, each of which therefore has eight monomers. The boundary between segments passes through the middle point of a link. The end monomer was ignored in the following analyses.

We have calculated segmental S for each segment. If the length (s_i) between two successive inflection points is larger than two segments, this was counted as belonging to the segment corresponding to the middle point of s_i. The temperature dependence of the segmental S at the respective segment is shown in Figure 16. In parallel with the behavior of S shown in the previous Section, the end-segment S decreases for $r_c = 1$, but increases for $r_c = 2$, as the temperature is lowered. The behaviors of all inner segments show a similar temperature dependence. There is a clear difference of the behaviors between the end segment and inner segments, that is, S is smaller for the end segment than for the inner segments.

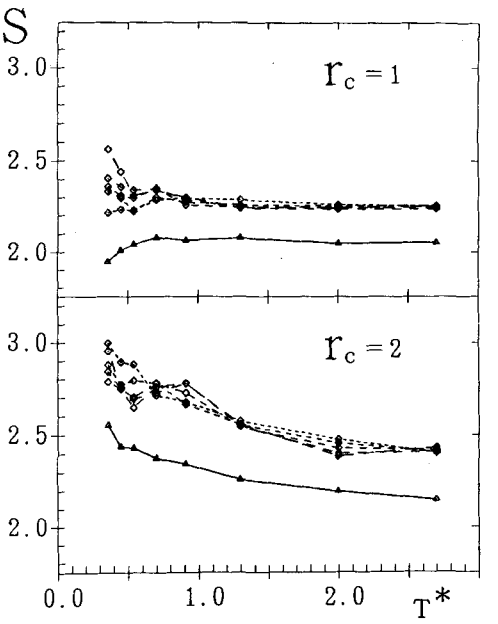

Figure 16 Temperature dependence of the segmental S for $r_c = 1$ and $r_c = 2$ with $N + 1 + 98$. Each curve is drawn as a guide to the eyes. △ is for the end segment, and □ is for the inner segments.

We also have calculated the persistence length L_p. For the square lattice model, we define L_p as:

$$L_p = \left\langle \frac{1}{K-1} \sum_{i=1}^{K-1} l_i \right\rangle \tag{10}$$

where l_i denotes the length between the $i-$th and $(i + 1)$th bend points. K is the total number of the bend points. Similarly to the segmental S, we calculated segmental L_p. The temperature dependence of the segmental L_p at the respective segment is shown in Figure 17. There is a similarity of the temperature dependence between L_p and S both for $r_c = 1$ and for $r_c = 2$. However, there is a remarkable difference between S and L_p for $r_c = 2$ below $T^* = 1$. In order to make clearer such a difference, the ratio, S/L_p, for the end segment is depicted in Figure 18. $\phi = (\pi/2)S/L_p$ can be interpreted as the turning angle caused by the rotation at every inflection measured from a fixed point. There are two remarkable points: first, ϕ is larger for $r_c = 1$ than for $r_c = 2$ except the lowest-temperature data. Secondly, ϕ increases rather rapidly, as the temperature is lowered, especially for the case of $r_c = 2$. Inner segments also show a similar temperature dependence of ϕ, but much less than that of the end segment. These results indicate that the chain is more preferably able to surround counterions in the end segment rather than in inner segments. This can be understood naturally, since the inner segments of the chain hardly surround counterions.

The winding angle θ is defined by the total angle of rotation along the chain:

$$\theta = \left\langle \left| \sum_{i=2}^{N} \theta_i \right| \right\rangle \tag{11}$$

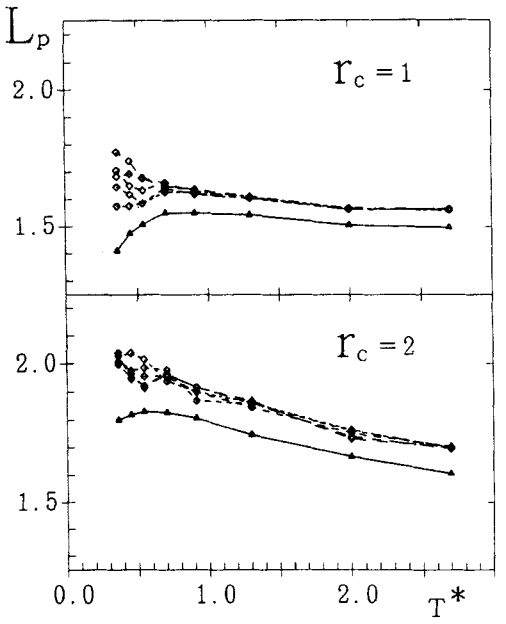

Figure 17 The temperature dependence of the segmental L_p for $r_c = 1$ and $r_c = 2$ with $N + 1 = 98$. Each curve is drawn as a guide to the eyes. △ is for the end segment, and □ is for the inner segments.

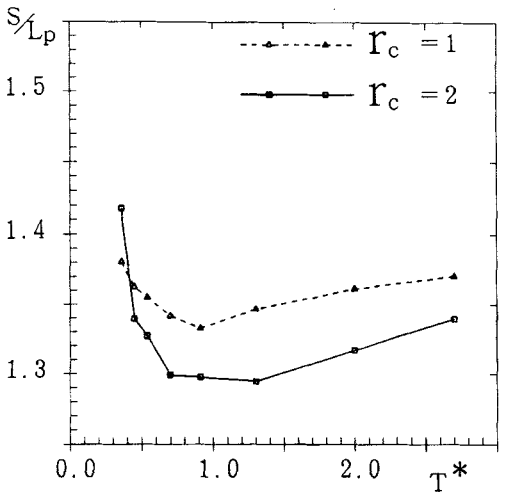

Figure 18 The temperature dependence of the ratio S/L_p for the end segment. Each curve is drawn as a guide to the eyes. △ is for $r_c = 1$, and □ is for $r_c = 2$.

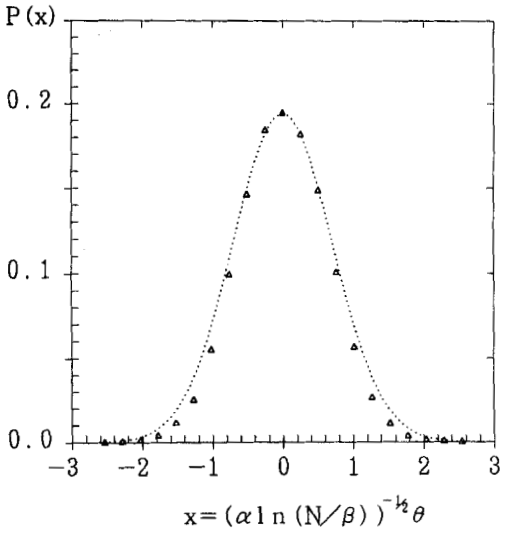

Figure 19 The distribution of winding angle for the neutral polymer chain with $N + 1 = 98$. α and β are obtained by the plots of θ^2 vs. $\ln(N)$ for the neutral polymer chain, so that $\alpha \sim 3.86$ and $\beta \sim 1.74$. The dotted curve is an exact gaussian distribution, $P(x) = P(0)\exp(-x^2)$ with $P(0)$ obtained by our simulations.

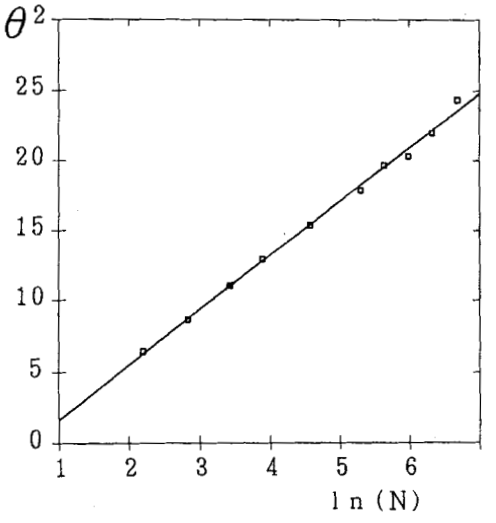

Figure 20 The plot of θ^2 vs. $\ln(N)$ for the neutral polymer chain. The line is obtained by a least-square fitting.

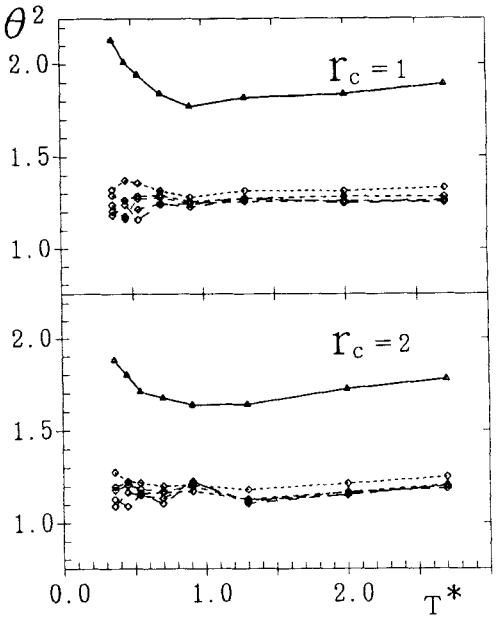

Figure 21 The temperature dependence of θ^2 for $r_c = 1$ and $r_c = 2$ with $N + 1 = 98$. Each curve is drawn as a guide to the eyes. △ is for the end-segment, and □ is for the inner segments.

where θ_i is the angle of rotation at the i − th monomer defined by the angle between the bond vectors $\mathbf{r}_{i+1} - \mathbf{r}_i$ and $\mathbf{r}_i - \mathbf{r}_{i-1}$ with $\theta_1 = \theta_{N+1} = 0$. It has been shown that for the neutral polymer chain, θ obeys the following scaling law [8]:

$$\theta \sim (\ln N)^{1/2} \tag{12}$$

We studied N-dependence of θ for a neutral polymer chain and a charged polymer chain via Monte Carlo simulations. For the neutral polymer case, we reconfirmed the Gaussian distribution of θ (see Figure 19), and a very good linear dependence between θ^2 and lnN (see Figure 20), equivalent to Equation (1), was obtained. For the charged polymer chain, however, the scaling relation of Equation (12) was not confirmed due to rather large statistical uncertainties of the data, especially in low temperatures. The Gaussian distribution of θ was partly confirmed. The segment-division analysis for the winding-angle was made. Equation (11) was used to calculate the segmental winding angle. The temperature dependence of segmental θ^2 for six different segments is shown in Figure 21. We see the clear difference of the behaviors between the end segment and the inner segments, for both $r_c = 1$ and $r_c = 2$. This difference was also affected for the neutral polymer chain. The θ^2 for inner segments show little temperature dependence. On the other hand, for the end segment, θ^2 increases rapidly below $T^* = 1$, for both $r_c = 1$ and $r_c = 2$.

4. DISCUSSION

We have performed Monte Carlo simulations for a single charged polymer chain

with counterions on the two-square-lattice model. Our system corresponds to a dilute limit case for polyelectrolytes with a sufficient number of salt ions so that chain-chain interactions can be neglected and the interactions between ions become short ranged. We used short-range logarithmic Coulomb interactions between any pairs of ions. Our attention was focused on the conformation characteristics of the chain, i.e., global, local, and segmental properties of the polymer chain. It has been shown that the conformation characteristics of the chain depend remarkably on the range of interaction between ions. The nearest-neighbor approximation ($r_c = 1$) shows little N dependence, and the Flory exponent υ is equivalent to that of the neutral polymer chain at each temperature. Both R_G and S are nearly constant at high temperatures, but those values tend to decrease as the temperature is lowered because of counterions condensation below $T^* = 1$. This condensation becomes remarkable as the temperature is lowered. These results suggest an order-disorder like change around $T^* = 1$ to take place. On the other hand, for the third-nearest-neighbor approximation ($r_c = 2$), υ substantially differs from that of the neutral polymer chain, and we found a remarkable N dependence for both R_G and S. As the length of the chain (N) becomes larger, observed changes around $T^* = 1$ are more remarkable. Thus, for a sufficiently larger N we predict a sharper transition, which can distinguish more clearly between the high-temperature and low-temperature phases.

We have found remarkable difference between the global and local conformation characteristics for $r_c = 2$. As the temperature is lowered down to around $T^* = 1$, the chain extends both more globally and more locally. However, as the temperature is further decreased ($T^* < 1$), the counterion condensation takes place dramatically, and as a result the chain contracts globally (R_G decreases), but the chain becomes more stiffened locally (S increases). Such a tendency becomes clearer as the temperature is lowered below $T^* = 1$.

The counterion condensation results in a notable difference between the end segment and the inner segments of the chain. In the inner segments of the chain, the counterions stick to the monomer. As a result, the inner parts of the chain tend to bend, rather than attempting to surround counterions. On the other hand, the end segment of the chain behaves differently, and is possible to surround near-neighbor counterions. This difference is more remarkable for $r_c = 2$ than for $r_c = 1$. Thus for a well branched chain, a strong counterions condensation may be possible.

The two-lattice model used in the present work significantly improved Monte Carlo simulations at low temperatures over the single-lattice model. However, it is still insufficient for very low temperatures and very long chains. Molecular dynamics simulations will not only be able to overcome some of these problems, but also be useful to study the dynamic properties of charged polymer chains [12]. Investigations for more realistic models, such as for three dimensional systems and/or for full Coulomb interactions (salt-free models) will be particularly of interest. The molecular dynamics simulation for a two-dimensional charged polymer chain is currently being undertaken.

Acknowledgment

The authors would like to thank Dr. V.M. Victor for valuable discussions and comments. This work is partially supported by a Grant-in-Aid from the Ministry of

Education, Science, and Culture, and also by Nissan Science Foundation. Computations were made using computers at the Information Process Center of Kanazawa University and the Plasma Institute of Nagoya University.

References

[1] J.M. Victor, J.P. Hansen, "On the form factor of two-dimensional polyelectrolytes under strong screening conditions". *Europhys. Lett.*, **3,** 1161 (1987).
[2] J.M. Victor. "The basic theory of polyelectrolytes", in The Physics and Chemistry of Aqueous Ionic Solutions, M.-C. Bellissent-Funel and G.W. Neilson eds. NATO ASI Series C Vol. 205, D. Reidel Publishing Company, 1987 pp. 291–310.
[3] G.S. Manning, "Limiting laws and counterion condensation in polyelectrolyte solutions I, colligative properties", *J. Chem. Phys.*, **51,** 924 (1969).
[4] J.P. Valleau, "Flexible polyelectrolyte in ionic solution: a Monte Carlo study", *Chem. Phys.*, **129,** 163 (1989).
[5] J. Takashima, M. Takasu, Y. Hiwatari, "Monte Carlo simulations of two-dimensional charged polymer chain", *Phys. Rev.*, **A40,** 2706 (1989).
[6] M. Takasu, J. Takashima, Y. Hiwatari, "A two-dimensional polymer chain with short-range interactions", in Strongly Coupled Plasma Physics, S. Ichimaru ed., Elsevier Science Publishers, 1990, pp. 679–682.
[7] K. Kaji, H. Urakawa, T. Kanaya, R. Kitamura. "Phase diagram of polyelectrolyte solutions", *J Phys. France.*, **49,** 993 (1988).
[8] B. Duplantier, H. Saleur, "Winding-angle distributions of two-dimensional self-avoiding walks from conformal invariance", *Phys. Rev. Lett.*, **60,** 2343 (1988).
[9] F. Mandel, "Macromolecular dimensions obtained by an efficient Monte Carlo method: the mean square end-to-end separation", *J. Chem. Phys.*, **70,** 3984 (1979).
[10] K. Binder, Monte Carlo Methods in Statistical Physics, Springer, New York, (1979).
[11] P.G. de Gennes. Scaling Concepts in Polymer Physics, Cornell University Press, Ithaca, (1979).
[12] K. Kremer, G.S. Grest, I. Carmesin, "Crossover from Rouse to reptation dynamics: a molecular dynamics simulation", *Phys. Rev. Lett.*, **61,** 566 (1988).